Surface Science 710 (2021) 121848

Contents lists available at ScienceDirect

Surface Science

journal homepage: www.elsevier.com/locate/susc

Self-assembly of ClAlPc molecules on moiré-patterned graphene grown on Pt(111)

Mariano D. Jiménez-Sánchez [a,*], Nour Sánchez-Abad [a], Nicoleta Nicoara [b], José M. Gómez-Rodríguez [a,c,d,1]

[a] Departamento de Física de la Materia Condensada, Universidad Autónoma de Madrid, E-28049 Madrid, Spain
[b] International Iberian Nanotechnology Laboratory (INL), 4715-330 Braga, Portugal
[c] Instituto Nicolás Cabrera, Universidad Autónoma de Madrid, E-28049 Madrid, Spain
[d] Condensed Matter Physics Center (IFIMAC), Universidad Autónoma de Madrid, E-28049 Madrid, Spain

ARTICLE INFO

Keywords:
Scanning Tunneling Microscopy
Graphene
Phthalocyanine
Molecular Self-Assembly

ABSTRACT

Phthalocyanines are promising molecules for the development of organic electronic devices, for instance, molecular heterojunctions in organic solar cells or organic field-effect transistors. For an optimum performance of these devices, the molecular ordering on the substrate and the molecular electronic level alignment have been shown as crucial factors. In this work, the self-assembled structure and the electronic structure of chloroaluminum phthalocyanines (ClAlPc) on graphene grown on Pt(111) surfaces have been studied by scanning tunneling microscopy (STM) under ultrahigh vacuum (UHV) and low-temperature conditions. Graphene grown on Pt(111) exhibits multiple moiré patterns with different periodicities, offering a benchmark to investigate the influence of the graphene and the moiré patterns in the ClAlPc ordering. This surface allows to extend previous works performed on graphite and graphene on Cu(100), where no moiré patterns are found. Well-ordered molecular islands exhibiting rotational domains have been observed in the submonolayer regime. The orientation of individual ClAlPc molecules within the structure unit cell has been characterized pointing out to a Cl-Up configuration adopted by the molecules. Our measurements show a correlation between the molecular lattice orientation and the graphene directions, whereas no influence of the underlying moiré patterns has been found. Finally, the ClAlPc electronic structure has been characterized indicating a weak graphene-molecule interaction.

1. Introduction

Phthalocyanines are a type of π-conjugated molecules which are promising for future applications in organic electronics [1-6]. One of these molecules is the chloroaluminum phthalocyanine (ClAlPc), which presents a non-planar structure with an intrinsic electric dipole perpendicular to its molecular π-plane [7-9]. ClAlPc has been proposed as a candidate for high-density data storage [10,11] and for molecular heterojunctions in organic solar cells in combination with the acceptor C_{60}, where ClAlPc behaves as the donor [12-14]. In the latter case, it has been demonstrated that the molecular electronic level alignment, which is strongly influenced by the molecular ordering, crucially determines the performance of the device [12,13,15]. Therefore, the characterization of the self-assembled structure of ClAlPc and its electronic structure is a relevant task since it would allow to choose the appropriate supporting substrate for molecules in the development of the devices of the incoming technology.

ClAlPc self-assembled structure has been studied mainly on metallic [16-19] and on highly oriented pyrolytic graphite (HOPG) surfaces [10, 13,19,20]. Similarities between previous studies have been found such as the self-assembled lattice symmetry and the individual ClAlPc adsorption geometry with the molecular π-plane lying parallel to the surface. Nevertheless, differences emerge from the molecule-substrate interaction on metal surfaces, where two dipole configurations in the as-grown first layer coexist, i.e. the electric dipole can be found pointing towards the substrate or towards the vacuum [16,18]. In contrast, on HOPG surfaces the first as-grown ClAlPc adlayer exhibits for all molecules the same dipole orientation, pointing towards the substrate. This dipolar alignment indicates that HOPG surfaces are appropriate substrates to achieve highly-ordered ClAlPc structures and that graphene

* Corresponding author.
E-mail address: marianod.jimenez@uam.es (M.D. Jiménez-Sánchez).
[1] Deceased on 1st November 2020.

https://doi.org/10.1016/j.susc.2021.121848
Received 18 January 2021; Received in revised form 23 March 2021; Accepted 24 March 2021
Available online 1 April 2021

surfaces could be also. Investigations about the ClAlPc assembly have been carried out on highly oriented pyrolytic graphite (HOPG) [10,13,19,20] and on graphene on Cu(100) (G/Cu(100)) [21], where the superstructures known as moiré patterns are not present. It is quite common however that graphene grown on a metallic substrate can lead to a non-uniform interaction with the underlying support. This interaction usually generates moiré patterns [22-26], which can induce changes in the molecular lattice symmetry, as it has been shown for other phthalocyanines [27-30]. To this respect, the characterization of the role played by the moiré patterns in the ClAlPc self-assembled structures could allow a more specific selection of the graphene-metal substrate for future applications. Other than this, regarding the electronic structure of ClAlPc on HOPG and graphene surfaces, up to our best knowledge, it has only been characterized by means of ultraviolet photoemission spectroscopy (UPS) on HOPG [7,8,13,16], and hence information about the unoccupied states of ClAlPc on HOPG and graphene surfaces is still missing in the literature.

In this work, we have undertaken the study of the self-assembled and the electronic structure of ClAlPc molecules adsorbed on graphene on Pt (111) surfaces (G/Pt(111)) by means of scanning tunneling microscopy (STM) under ultrahigh vacuum (UHV) and low temperature (40 K and 5 K) conditions. G/Pt(111) was chosen due to the low graphene-metal interaction [31-33] as well as the multiple moiré patterns forming on the surface [22,33-35]. On the other side, the ClAlPc non-planar structure, which differs from the planar phthalocyanines explored on graphene surfaces [27,29], could provide information on the molecule-graphene interaction since ClAlPc can adopt different adsorption configurations on the surface. The obtained results show the growth of well-ordered single-layer islands of ClAlPc where the molecules presumably adopt a Cl-Up configuration with their dipole pointing towards the substrate. By means of high-resolution images, the inner structure of the molecular cell has been resolved and the influence of the graphene high-symmetry directions in the molecular ordering has been unveiled. However, no influence of the underlying moiré patterns in the molecular lattice symmetry or orientation has been found. Finally, the ClAlPc electronic structure has been characterized by obtaining information about the frontier orbitals that indicates a low molecule-graphene interaction.

2. Experimental section

The experiments have been carried out in two different UHV systems (base pressure $\sim 1 \times 10^{-10}$Torr. Both systems consist of two chambers: a preparation and an analysis chamber. The preparation chambers are equipped with standard devices for sample cleaning and growth of epitaxial graphene under UHV conditions. The analysis chambers differ between the systems. One of them is endowed with a home-made variable temperature scanning tunneling microscope (VT-STM) able to operate from 40 K to 400 K [36]. The VT-STM has been employed to perform measurements at 40 K of the ClAlPc self-assembled structure on G/Pt(111). The second analysis chamber is equipped with a home-made non-contact Atomic Force Microscopy ncAFM/STM able to operate at 5 K [32]; this system has been employed as STM to acquire data at low-temperature (5 K). Conductance measurements have been obtained with the 5 K microscope by means of a lock-in technique with an AC voltage ($f_0 = 836$ Hz, $V_{amplitude} = 10$ mV) added to the DC bias voltage. In both microscopes electrochemically etched W tips have been employed and the bias voltages are referred to the sample. STM data acquisition and processing have been performed with the WSxM software.

The cleaning process of the Pt(111) single crystal was performed by means of cycles of Ar^+ sputtering at 1 kV and annealing at 1070 K in presence of oxygen atmosphere (10^{-7}Torr). After each cycle, the sample was flashed at 1270 K in presence of the same oxygen atmosphere. Once the cleaning cycles were completed, the graphene was grown through ethylene chemical vapor deposition (CVD) by exposing the surface to 60 L while it was held at 1270 K. The quality of the graphene layer was checked by means of STM measurements at room temperature (RT). ClAlPc molecules were evaporated onto the G/Pt(111) surface at RT using a home-made Ta crucible heated at ~350 °C. The deposition rate was 0.7 ML/min as calibrated by means of a quartz balance. The evaporation time was selected in order to achieve a submonolayer coverage of the sample. During the deposition rate calibration, coverages over the monolayer have been obtained (See supporting information for further details). Prior to STM measurements, the sample was cooled down to low temperature in order to prevent the diffusion of the ClAlPc molecules.

3. RESULTS AND DISCUSSION

Graphene grown on Pt(111) surfaces presents a large number of rotational domains due to the low graphene-metal interaction of this interface. Consequently, several moiré patterns are present, i.e. different periodicities of the graphene superstructure can be found on these surfaces. Although these superperiodicities have been previously reported [22,33-35], for an easy and self-consistent understanding of the results, two examples of moiré patterns associated to two different graphene-metal rotations are shown in fig. 1. The atomically resolved STM image showed in fig. 1a presents a moiré pattern with a periodicity of ~2 nm and a structure $[(\sqrt{67} \times \sqrt{67}) - R12.2^\circ]_G$ with respect to the graphene or, equivalently, a structure $[(2\sqrt{13} \times 2\sqrt{13}) - R13.9^\circ]_{Pt}$ referred to the Pt(111). A geometric model of this moiré pattern is shown in fig. 1b, where the graphene layer is rotated 1.7° with respect to the underlying Pt(111) and the green and the grey spheres represent the

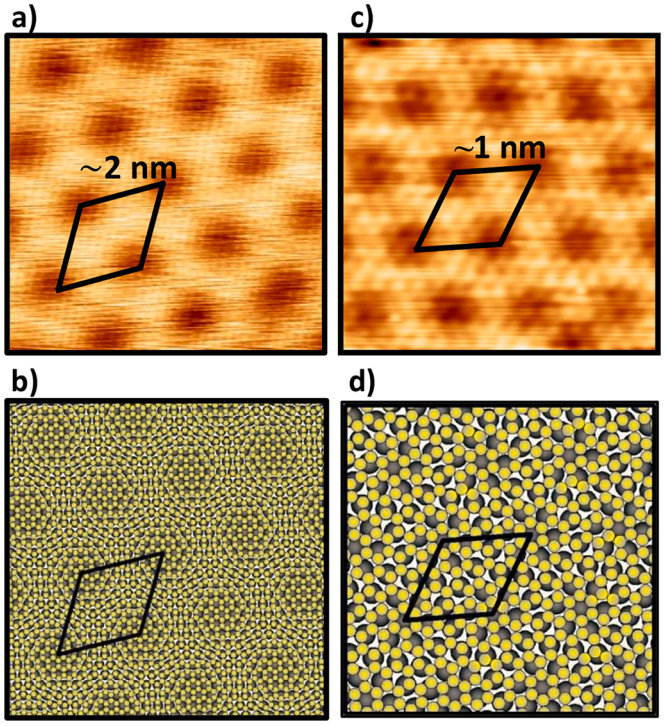

Fig. 1. STM images measured at room temperature exhibiting examples of different moiré patterns of the G/Pt(111) surface. The moiré unit cells are outlined in black. a) $[(\sqrt{67} \times \sqrt{67}) - R12.2^\circ]_G$, referred to graphene, or, equivalently, $[(2\sqrt{13} \times 2\sqrt{13}) - R13.9^\circ]_{Pt}$, with respect to Pt(111). Image size: 7.5 × 7.5 nm^2; V_s = -20 mV, I = 18 nA. b) Schematic model of the moiré pattern displayed in a). Green and grey spheres represent the graphene and Pt atoms, respectively. c) $[(4 \times 4)]_G$, referred to graphene, or, equivalently, $[(\sqrt{13} \times \sqrt{13}) - R13.9^\circ]_{Pt}$, with respect to Pt(111). Image size: 3.7 × 3.7 nm^2; V_s = 0.9 V, I = 1 nA. d) Schematic model of the moiré pattern in c). The color code is the same as in b).

graphene and the Pt atoms, respectively. The atomically resolved STM image in fig. 1c, acquired in a different sample region displays a different periodicity of the graphene superstructure (~1 nm), originated by a rotation of 13.9° of the carbon layer with respect to the substrate. This moiré can be noted as $[(4 \times 4)]_G$ with respect to the graphene or as $[(\sqrt{13} \times \sqrt{13}) - R13.9°]_{Pt}$ with respect to the Pt(111). A geometric model of this moiré is displayed in fig. 1d following the same color code as for the model in fig. 1b. These moiré patterns and their geometric structures displayed in fig. 1 have been previously described [22,35]. Although they are found on the surface with a similar abundance to other moiré patterns, they are shown here as they exemplify the variety of moiré patterns present at this surface. This diversity makes G/Pt(111) an excellent interface for the investigation of the substrate influence in the molecular adlayer ordering. As shown, each superperiodicity presents different relative orientations between the moiré and the graphene lattices, and hence, the exploration of the molecule adsorption on top of different moiré patterns would unveil the role played by each periodicity in the molecular lattice structure.

Chloroaluminum phthalocyanine (ClAlPc) molecule, with structural formula $C_{32}H_{16}AlClN_8$, presents a cross-shaped structure with a chlorine atom protruding the molecular π-plane, which gives rise to an electric dipole pointing towards the molecular plane. Such structure can be visualized in fig. 2a-b, where a top and side view are displayed respectively, following the atomic coordinates obtained from the characterization of a ClAlPc single crystal by K. J. Wynne [37]. Fig. 2c-d show typical STM images acquired on the G/Pt(111) surface at 40 K, after the deposition of ClAlPc molecules at room temperature (RT), following the procedure described in the experimental section. The submonolayer coverage leads to molecular islands coexisting with bare graphene regions, as those imaged in fig. 2c, where the uncovered graphene is indicated by "G" and the molecular islands by "ClAlPc". It can be observed that molecules tend to self-assemble into two-dimensional well-ordered islands. The symmetry of these single-layer islands can be observed in fig. 2d, which corresponds to a zoom in the region indicated with a square in fig. 2c. This zoom reveals a lattice of bright spots protruding outwards the molecule layer exhibiting a square unit cell, outlined in black, with a lattice parameter of ~1.5 nm. These molecular islands have been found to exhibit several relative rotations between them. Nevertheless, a closer inspection has revealed that, over a given graphene flake, only 30° rotations between the lattice directions of different islands are present. An example of these rotations is shown in fig. 2e.

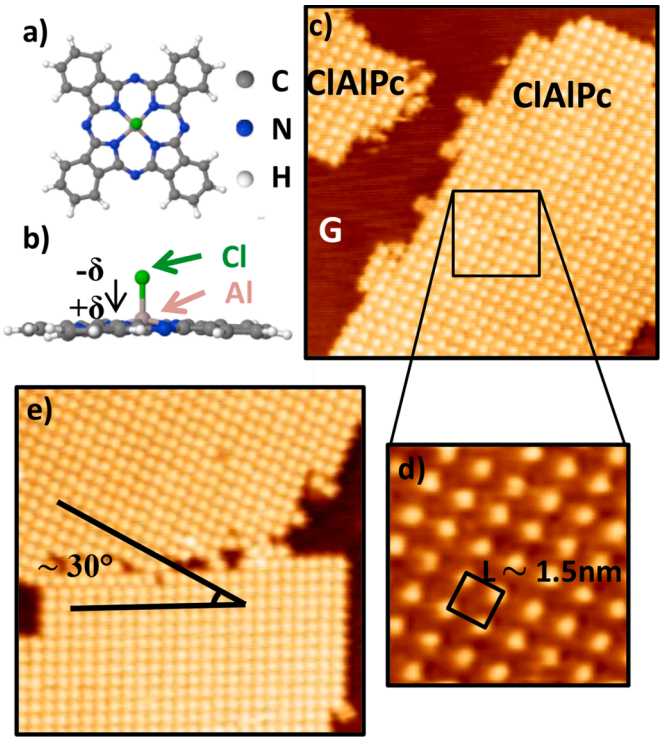

Fig. 2. STM images of ClAlPc molecules on G/Pt(111) acquired at 40 K. a) and b) display the top and side view of the ClAlPc structure respectively. The electric dipole is depicted by the black arrow. c) Image of single-layer ClAlPc islands coexisting with bare graphene areas (G). Image size: 40 × 40 nm^2; tunneling parameters: V_s = 3 V; I_t = 50 pA. d) Zoom-in in the indicated region of c) showing the squared unit cell of the molecular island with a lattice parameter L. Image size: 10 × 10 nm^2; tunneling parameters: V_s = 3 V; I_t = 50 pA. e) STM image showing molecular domains, rotated 30, found over the same graphene flake. Image size: 40 × 40 nm^2; tunneling parameters: V_s = 2.7 V; I_t = 10 pA.

In order to elucidate the origin of the bright spots as those observed in fig. 2d and the molecular adsorption geometry on the graphene substrate, STM images where the molecular cross shape is resolved were acquired within ClAlPc islands in different regions; an example is shown in fig. 3. The comparison of this image with the ClAlPc structure, superimposed in the STM image, unveils details about the adsorption geometry on the substrate and the molecular orientation within the unit cell, marked with a black square. In fig. 3 the ClAlPc cross-shape can be easily identified, revealing that the molecule is lying down flat with the molecular π-plane parallel to the graphene. Furthermore, the rotation of each molecule with respect to the molecular lattice direction can be measured. Attending to our observations the angle between the ClAlPc high-symmetry direction (blue line) and the molecular lattice direction (red line) is ~30°. The comparison of fig. 3 with previously reported STM images of ClAlPc on other substrates suggests that the observed bright spots correspond to the chlorine atom [10,13,18,21,38,39]. This plausible identification of the chlorine atom is also supported by the apparent height of the bright spots and by STM images of the ClAlPc bilayer, where the first and second layers are visualized simultaneously and the bright spots in the second layer are absent (see the Supporting Information for more details). Thus, the ClAlPc molecules are presumably adsorbed in a Cl-Up configuration in which the chlorine atom points towards the vacuum and the electric dipole towards the graphene (see inset in fig. 3). This likely Cl-Up configuration would indicate the

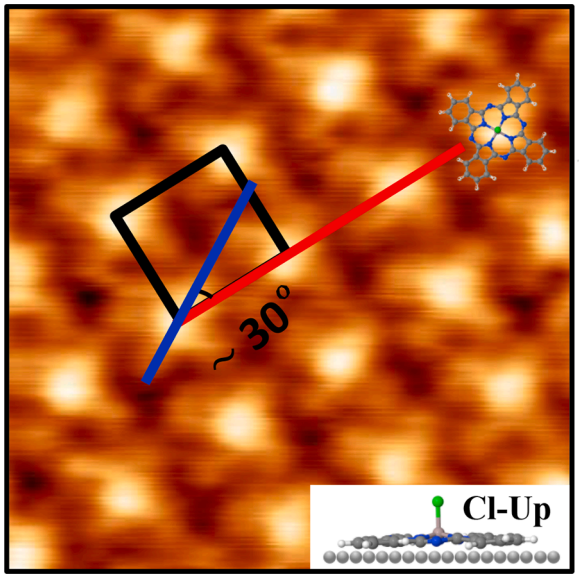

Fig. 3. STM image obtained in a single-layer ClAlPc island showing the individual molecular orientation within the lattice unit cell. ClAlPc structure is superimposed in the image. The molecular unit cell is indicated by the black square. The high-symmetry direction of the molecule is outlined with a blue line. The red line marks the molecular lattice direction. Image size: 7 × 7 nm^2; tunneling parameters: V_s = -1.5 V; I_t = 80 pA.

relevance of the molecular plane-substrate interaction in the adsorption process as it maximizes the π-π interaction between the ClAlPc molecules and the underlying carbon surface [20,21]. Following the identification of the molecular bright spot with the chlorine atom, the molecules in fig. 2c and fig. 2e which do not display such bright spot could correspond to molecules which have lost the chlorine atom or to molecules placed in Cl-Down configuration, i.e. with the electric dipole pointing towards the vacuum.

The influence of the underlying substrate (moiré pattern and graphene lattice) in the molecular ordering has been also investigated. To shed light on this issue, STM images have been acquired close to the ClAlPc island borders between the molecular single-layer and the adjacent uncovered graphene. By combining the images from both locations, the high-symmetry directions of the molecular island, the moiré pattern and the graphene lattice can be obtained, as well as the angle between them. Fig. 4 displays examples of these measurements on different graphene flakes. Fig. 4a, b and c show STM images of ClAlPc islands close to their borders where the molecular lattice direction is outlined with a red line. Fig. 4d, e and f correspond to topographies acquired in the uncovered graphene areas indicated with a white square in fig. 4a, b and c, respectively. In these graphene images, the high-symmetry direction of graphene is outlined with a black line and the moiré unit cell is highlighted in blue. The insets show the angle measured between the molecular lattice (red) and the graphene directions (black). In our experiments rotations of ~15° and ~45° between the graphene directions and the ClAlPc lattice directions have been found. However, neither the ClAlPc lattice symmetry nor the orientations with respect to the substrate have shown any dependence on the underlying moiré patterns or the Pt(111) substrate. Considering the general morphology of the ClAlPc islands, i.e. shape and size, remarkable differences that could be attributable to the different underlying moiré patterns have not been observed.

The observed behavior of the ClAlPc self-assembled lattices are in close resemblance with the results obtained from ClAlPc deposition onto HOPG [20] and G/Cu(100) [21] surfaces, where no moiré patterns were observed. This indicates that the molecule-substrate interaction is mainly determined by the graphene lattice and not by the moiré pattern. The weak influence of the G/Pt(111) moiré patterns differs from other graphene/metal substrates where the deposition of phthalocyanines can lead to non-squared lattices governed by the moiré pattern [27-30]. The ClAlPc self-assembly independence on the underlying moiré in the G/Pt (111) interface can be attributed to the decoupling of the graphene from the metal substrate, giving rise to low corrugated moiré patterns with a low perturbed graphene electronic structure [31-33].

By combining the results obtained in different sample regions about the ClAlPc orientation within the molecular unit cell (fig. 3) and the orientation of the unit cell with respect to the substrate (fig. 4), an adsorption model is proposed for the ClAlPc/G/Pt(111) system. In this model, shown in fig. 5, the (11) direction of the ClAlPc lattice (the diagonal of the cell) is parallel to one of the high-symmetry directions of the graphene, as observed in fig. 4. On the other hand, taking into account STM images where the molecular cross shape is resolved, as the one shown in fig. 3, the ClAlPc symmetry direction of each molecule is

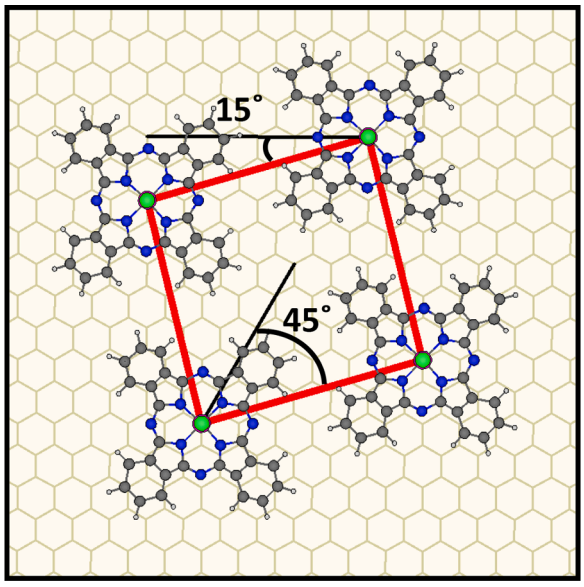

Fig. 5. Geometric model proposed for the adsorption of ClAlPc molecules on G/Pt(111). The graphene is represented by the brown honeycomb structure and two of its high-symmetry directions are indicated with black lines. The ClAlPc unit cell is outlined in red.

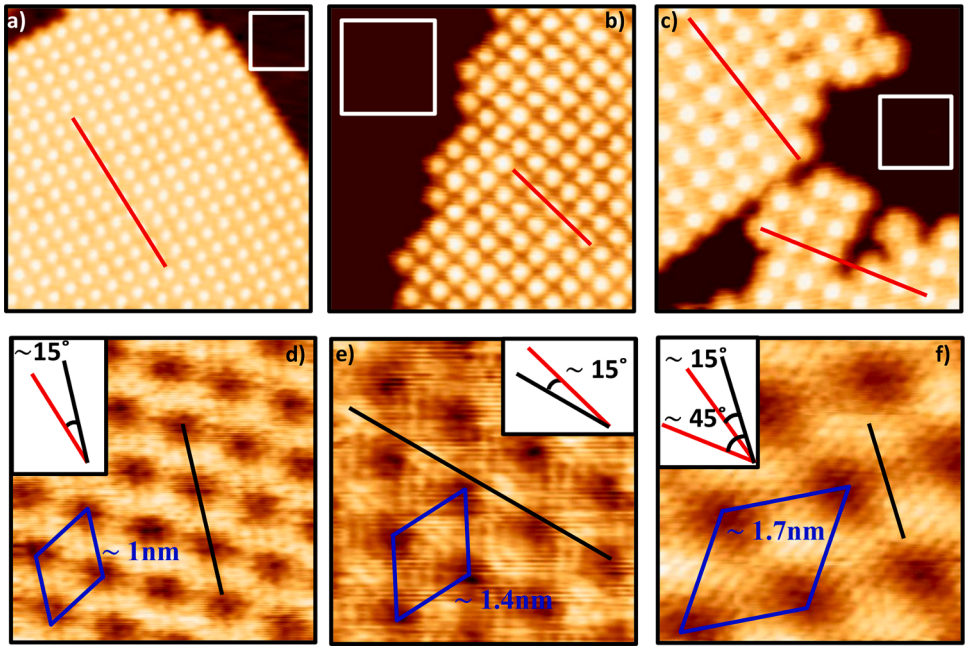

Fig. 4. Representative STM images of the study of the graphene influence on the molecular ordering. a), b) and c) present images of single-layer ClAlPc islands close to their border. The red lines indicate the molecular lattice direction. d), e) and f) show atomically resolved images of the graphene areas marked with a white square in a), b) and c), respectively. The unit cell and periodicity of the different moiré patterns observed are indicated in blue. The black lines outline the graphene lattice direction. The insets show the measured angle between the molecular lattice direction (red) and the graphene direction (black). Size image: a) 25 × 25 nm^2; b) 15 × 15 nm^2; c) 20 × 20 nm^2; d), e) and f) 5 × 5 nm^2. Tunneling parameters: a) V_s = 3 V; I_t = 10 pA; b) V_s = 2.5 V; I_t = 10 pA; c) V_s = 2.5 V; I_t = 8 pA; d) V_s = -50 mV; I_t = 17 nA; e) V_s = 0.2 V; I_t = 15 nA; f) V_s = -0.15 V; I_t = 3.8 nA.

rotated 30° with respect to the molecular lattice direction. Based on this model, the measured 15° and 45° relative angles between the graphene directions (black lines) and the ClAlPc lattice directions (red lines) in fig. 4 are reconstructed. Regarding the 30° angles found between ClAlPc islands on the same graphene flake (fig. 2e and fig. 4c), they can be explained as rotational domains following the proposed model, i.e. as molecular lattices where (11) direction is aligned with different high-symmetry directions of the graphene (for further details see Supplementary Information).

Finally, the electronic structure of ClAlPc adsorbed on G/Pt(111) has been characterized by means of scanning tunneling spectroscopy (STS) at 5 K. Conductance curves (dI/dV) have been acquired on top of individual ClAlPc molecules; a representative example of these measurements is shown in fig. 6a. This spectrum, which has been acquired at the center of a molecule, shows a gap of ~2.7 V flanked by two peaks whose centers are located at ~-1.25 V and ~+1.5 V (the bias voltage is applied to the sample). These peaks can be associated to the frontier orbitals of the molecule, i.e. to the highest occupied molecular orbital (HOMO) and the lowest unoccupied molecular orbital (LUMO). STM images, shown in fig. 6b and c, have been acquired at 5 K at bias voltages close to the HOMO and LUMO peaks obtained in the conductance curve, respectively. These images, where the individual ClAlPc orientation is indicated with a dotted cross, reveal the presence of intramolecular features, which depend on the applied bias. Single-molecule intramolecular features have been marked with colored dots to facilitate their identification. In fig. 6b, obtained for a bias voltage close to the HOMO energy position, it can be observed that the molecular center exhibits a depression while the molecular cross shape presents four lobes per branch, indicated with a total of sixteen blue dots. In fig. 6c, obtained for a bias voltage close to the LUMO energy position, it can be observed that each branch of the molecular cross shape shows two lobes, indicated all of them with a total of eight red dots, while the area around the molecular center presents a larger electronic contribution, i.e. a higher apparent height, with respect to the depicted lobes. It is also remarkable that for the latter case the molecular center also exhibits a subtle depression.

The energy value found for the peak below the Fermi level (negative bias) in fig. 6a is in good agreement with previous values, between -1.2 and -1.3 eV, obtained by ultraviolet photoemission spectroscopy for the HOMO orbital of ClAlPc first layers adsorbed on graphite surfaces [7,8,13,16]. This agreement reinforces the identification of this peak with the HOMO orbital and suggests a comparable ClAlPc-substrate interaction on HOPG and G/Pt(111) systems. Furthermore, the peak above the Fermi level (positive bias), up to our best knowledge, constitutes the first reported value for the ClAlPc LUMO orbital on HOPG or graphene surfaces. The intramolecular structures observed in fig. 6b and c present similarities with the structures previously reported by DFT calculations for the free-molecule HOMO and LUMO orbitals [38]. In the HOMO case, the similarities are the four lobes in each molecular branch and the central depression of the molecule. With respect to the LUMO, the main resemblances are the larger electronic contribution around the molecular center with respect to the molecular branches and the lower electronic contribution at the molecular center which could be associated with the subtle central depression in fig. 6c. All these similarities point towards a weak molecule-graphene interaction [35].

4. Conclusions

In this work, we have investigated the ClAlPc self-assembled structure in the submonolayer regime on graphene grown on Pt(111) substrates by using low-temperature STM. According to our results, ordered single-layer islands are formed on the surface, where the molecules likely adopt a Cl-Up configuration in close resemblance to HOPG and G/Cu(100) surfaces where no moiré patterns are present. The orientation of the ClAlPc within the molecular islands and the influence of the substrate in such layers have been characterized. Graphene high-symmetry directions have been found to be determinant in the alignment of the ClAlPc islands, while no influence of the underlying moiré pattern or the metal substrate has been observed. In addition, an adsorption model for ClAlPc on G/Pt(111) has been proposed based on the obtained results. Furthermore, the electronic structure around the Fermi level has been explored by STS and peaks related to the HOMO and LUMO were observed. Finally, STM images have been acquired at a bias close to the frontier orbital values found, revealing intramolecular features.

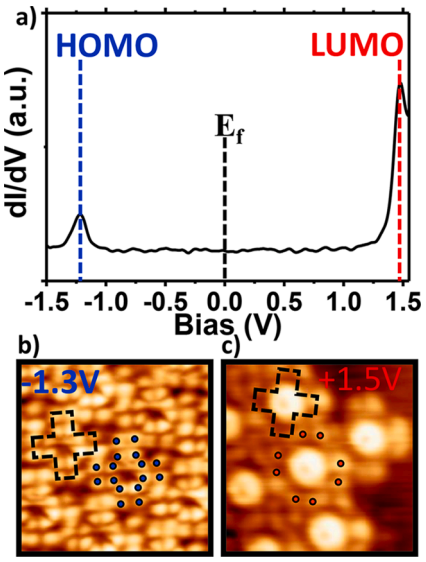

Fig. 6. ClAlPc electronic structure characterization. a) Conductance curve acquired on a ClAlPc molecule at 5 K. The bias is applied to the sample. The HOMO and LUMO peaks and the Fermi level (E_f) are indicated. b) STM image of a ClAlPc island acquired at 5 K at the HOMO bias. The individual molecular orientation is marked by a dashed cross. The blue dots indicate the intramolecular features of a single molecule. Image size: 4 × 4 nm^2; tunneling parameters: V_s = -1.3 V; I_t = 70 pA. c) STM image of a ClAlPc island acquired at 5 K at the LUMO bias. The individual molecular orientation is marked by a dashed cross. The red dots indicate the intramolecular features of a single molecule. Image size: 4 × 4 nm^2; tunneling parameters: V_s = +1.5 V; I_t = 80 pA.

CRediT authorship contribution statement

Mariano D. Jiménez-Sánchez: Investigation, Visualization, Writing – original draft, Writing – review & editing. **Nour Sánchez-Abad:** Investigation, Writing – review & editing. **Nicoleta Nicoara:** Resources, Writing – review & editing. **José M. Gómez-Rodríguez:** Conceptualization, Writing – review & editing, Supervision, Funding acquisition.

Declaration of Competing Interest

The authors declare that they have no known competing financial interests or personal relationships that could have appeared to influence the work reported in this paper.

Acknowledgments

Financial support from the Spanish Ministerio de Economía y Competitividad (MINECO) and Fondo Europeo de Desarrollo Regional (FEDER) under grant No. MAT2016-77852-C2-2-R and from the Spanish Ministerio de Ciencia e Innovación, through the "María de Maeztu" Programme for Units of Excellence in R&D (grant No. CEX2018-000805-M) is gratefully acknowledged.

Supplementary materials

Supplementary material associated with this article can be found, in the online version, at doi:10.1016/j.susc.2021.121848.

References

[1] T.V. Basova, E.K. Kol'tsov, I.K. Igumenov, Spectral investigation of interaction of copper phthalocyanine with nitrogen dioxide, Sensors and Actuators B-Chemical 105 (2005) 259–265.

[2] N.R. Armstrong, W.N. Wang, D.M. Alloway, D. Placencia, E. Ratcliff, M. Brumbach, Organic/Organic' Heterojunctions: Organic Light Emitting Diodes and Organic Photovoltaic Devices, Macromol. Rapid Commun. 30 (2009) 717–731.

[3] D. Song, F. Zhu, B. Yu, L.H. Huang, Y.H. Geng, D.H. Yana, Tin (IV) phthalocyanine oxide: An air-stable semiconductor with high electron mobility, Applied Physics Letters 92 (2008), 143303.

[4] L.Q. Li, Q.X. Tang, H.X. Li, X.D. Yang, W.P. Hu, Y.B. Song, Z.G. Shuai, W. Xu, Y. Q. Liu, D.B. Zhu, An ultra closely pi-stacked organic semiconductor for high performance field-effect transistors, Adv. Mater. 19 (2007) 2613.

[5] F. Pan, H.K. Tian, X.R. Qian, L.Z. Huang, Y.H. Geng, D.H. Yan, High performance vanadyl phthalocyanine thin-film transistors based on fluorobenzene end-capped quaterthiophene as the inducing layer, Organic Electronics 12 (2011) 1358–1363.

[6] O.A. Melville, B.H. Lessard, T.P. Bender, Phthalocyanine-Based Organic Thin-Film Transistors: A Review of Recent Advances, ACS Appl. Mater. Interfaces 7 (2015) 13105–13118.

[7] S. Kera, H. Yamane, H. Honda, H. Fukagawa, K.K. Okudaira, N. Ueno, Photoelectron fine structures of uppermost valence band for well-characterized ClAl-phthalocyanine ultrathin film: UPS and MAES study, Surf Sci 566 (2004) 571–578.

[8] H. Fukagawa, S. Hosoumi, H. Yamane, S. Kera, N. Ueno, Dielectric properties of polar-phthalocyanine monolayer systems with repulsive dipole interaction, Physical Review B 83 (2011), 085304.

[9] F. Latteyer, H. Peisert, U. Aygul, I. Biswas, F. Petraki, T. Basova, A. Vollmer, T. Chasse, Laterally Resolved Orientation and Film Thickness of Polar Metal Chlorine Phthalocyanines on Au and ITO, J. Phys. Chem. C 115 (2011) 11657–11665.

[10] Y.L. Huang, Y. Lu, T.C. Niu, H. Huang, S. Kera, N. Ueno, A.T.S. Wee, W. Chen, Reversible Single-Molecule Switching in an Ordered Monolayer Molecular Dipole Array, Small 8 (2012) 1423–1428.

[11] J.L. Zhang, J.L. Xu, T.C. Niu, Y.H. Lu, L. Liu, W. Chen, Reversible Switching of a Single-Dipole Molecule Imbedded in Two-Dimensional Hydrogen-Bonded Binary Molecular Networks, J. Phys. Chem. C 118 (2014) 1712–1718.

[12] S. Zhong, J.Q. Zhong, X.Z. Wang, M.Y. Huang, D.C. Qi, Z.K. Chen, W. Chen, Investigation of Interface Properties for ClAlPc/C-60 Heterojunction-Based Inverted Organic Solar Cell, J. Phys. Chem. C 116 (2012) 2521–2526.

[13] H.Y. Mao, R. Wang, Y. Wang, T.C. Niu, J.Q. Zhong, M.Y. Huang, D.C. Qi, K.P. Loh, A.T.S. Wee, W. Chen, Chemical vapor deposition graphene as structural template to control interfacial molecular orientation of chloroaluminium phthalocyanine, Applied Physics Letters 99 (2011), 093301.

[14] N. Beaumont, I. Hancox, P. Sullivan, R.A. Hatton, T.S. Jones, Increased efficiency in small molecule organic photovoltaic cells through electrode modification with self-assembled monolayers, Energy & Environmental Science 4 (2011) 1708–1711.

[15] J.L. Zhang, X. Ye, C.D. Gu, C. Han, S. Sun, L. Wang, W. Chen, Non -covalent interaction controlled 2D organic semiconductor films: Molecular self -assembly, electronic and optical properties, and electronic devices, Surf. Sci. Rep. 75 (2020), 100481.

[16] Y.L. Huang, W. Chen, F. Bussolotti, T.C. Niu, A.T.S. Wee, N. Ueno, S. Kera, Impact of molecule-dipole orientation on energy level alignment at the submolecular scale, Physical Review B 87 (2013) 6.

[17] T. Niu, Surface strain mediated dipole alignment of ClAlPc on Au(111), Applied Physics Letters 106 (2015), 161601.

[18] S. Matencio, R. Palacios-Rivera, J.I. Martinez, C. Ocal, E. Barrena, Chiral Organization and Charge Redistribution in Chloroaluminum Phthalocyanine on Au (111) Beyond the Monolayer, J. Phys. Chem. C 122 (2018) 16033–16041.

[19] T.C. Niu, N. Si, D.C. Zhou, M. Zhou, Submolecular Imaging of Parallel Offset pi-pi Stacking in Nonplanar Phthalocyanine Bilayers, J. Phys. Chem. C 123 (2019) 7178–7184.

[20] Y.L. Huang, R. Wang, T.C. Niu, S. Kera, N. Ueno, J. Pflaum, A.T.S. Wee, W. Chen, One dimensional molecular dipole chain arrays on graphite via nanoscale phase separation, Chemical Communications 46 (2010) 9040–9042.

[21] Y. Ogawa, T. Niu, S.L. Wong, M. Tsuji, A.T.S. Wee, W. Chen, H. Ago, Self-Assembly of Polar Phthalocyanine Molecules on Graphene Grown by Chemical Vapor Deposition, J. Phys. Chem. C 117 (2013) 21849–21855.

[22] P. Merino, M. Svec, A.L. Pinardi, G. Otero, J.A. Martín-Gago, Strain-Driven Moire Superstructures of Epitaxial Graphene on Transition Metal Surfaces, ACS Nano 5 (2011) 5627–5634.

[23] A. Martín-Recio, C. Romero-Muñiz, A.J. Martínez-Galera, P. Pou, R. Pérez, J. M. Gómez-Rodríguez, Tug-of-war between corrugation and binding energy: revealing the formation of multiple moire patterns on a strongly interacting graphene-metal system, Nanoscale 7 (2015) 11300–11309.

[24] J. Wintterlin, M.L. Bocquet, Graphene on metal surfaces, Surf Sci 603 (2009) 1841–1852.

[25] A.T. N'Diaye, J. Coraux, T.N. Plasa, C. Busse, T. Michely, Structure of epitaxial graphene on Ir(111), New J. Phys. 10 (2008), 043033.

[26] M. Batzill, The surface science of graphene: Metal interfaces, CVD synthesis, nanoribbons, chemical modifications, and defects, Surf. Sci. Rep. 67 (2012) 83–115.

[27] J.H. Mao, H.G. Zhang, Y.H. Jiang, Y. Pan, M. Gao, W.D. Xiao, H.J. Gao, Tunability of Supramolecular Kagome Lattices of Magnetic Phthalocyanines Using Graphene-Based Moire Patterns as Templates, J. Am. Chem. Soc. 131 (2009) 14136.

[28] H.G. Zhang, J.T. Sun, T. Low, L.Z. Zhang, Y. Pan, Q. Liu, J.H. Mao, H.T. Zhou, H. M. Guo, S.X. Du, F. Guinea, H.J. Gao, Assembly of iron phthalocyanine and pentacene molecules on a graphene monolayer grown on Ru(0001), Physical Review B 84 (2011), 245436.

[29] N. Neel, J. Kroger, Template Effect of the Graphene Moire Lattice on Phthalocyanine Assembly, Molecules 22 (2017) 731.

[30] H.G. Zhang, W.D. Xiao, J.H. Mao, H.T. Zhou, G. Li, Y. Zhang, L.W. Liu, S.X. Du, H. J. Gao, Host-Guest Superstructures on Graphene-Based Kagome Lattice, J. Phys. Chem. C 116 (2012) 11091–11095.

[31] P. Sutter, J.T. Sadowski, E. Sutter, Graphene on Pt(111): Growth and substrate interaction, Physical Review B 80 (2009), 245411.

[32] B. de la Torre, M. Ellner, P. Pou, N. Nicoara, R. Pérez, J.M. Gómez-Rodríguez, Atomic-Scale Variations of the Mechanical Response of 2D Materials Detected by Noncontact Atomic Force Microscopy, Phys. Rev. Lett. 116 (2016), 245502.

[33] M.M. Ugeda, D. Fernandez-Torre, I. Brihuega, P. Pou, A.J. Martínez-Galera, R. Pérez, J.M. Gómez-Rodríguez, Point Defects on Graphene on Metals, Phys. Rev. Lett. 107 (2011), 116803.

[34] A.J. Martínez-Galera, J.M. Gómez-Rodríguez, Surface Diffusion of Simple Organic Molecules on Graphene on Pt(111), J. Phys. Chem. C 115 (2011) 23036–23042, b.

[35] A.J. Martínez-Galera, N. Nicoara, J.I. Martínez, Y.J. Dappe, J. Ortega, J.M. Gómez-Rodríguez, Imaging Molecular Orbitals of PTCDA on Graphene on Pt(111): Electronic Structure by STM and First-Principles Calculations, J. Phys. Chem. C 118 (2014) 12782–12788.

[36] O. Custance, S. Brochard, I. Brihuega, E. Artacho, J.M. Soler, A.M. Baro, J. M. Gomez-Rodriguez, Single adatom adsorption and diffusion on Si(111)-(7x7) surfaces: Scanning tunneling microscopy and first-principles calculations, Physical Review B 67 (2003), 235410.

[37] K.J. Wynne, CRYSTAL AND MOLECULAR-STRUCTURE OF CHLORO (PHTHALOCYANINATO)GALLIUM(III), GA(PC)CL, AND CHLORO (PHTHALOCYANINATO)ALUMINUM(III), AL(PC)CL, Inorganic Chemistry 23 (1984) 4658–4663.

[38] T. Niu, M. Zhou, J. Zhang, Y. Feng, W. Chen, Dipole Orientation Dependent Symmetry Reduction of Chloroaluminum Phthalocyanine on Cu(111), J. Phys. Chem. C 117 (2013) 1013–1019.

[39] H.J. Song, C.F. Fu, N. Li, H. Zhu, Z.T. Peng, W.H. Zhao, J.X. Dai, L.B. Xing, Z. C. Huang, W. Chen, Y.F. Wang, J.L. Yang, K. Wu, On the shuttling mechanism of a chlorine atom in a chloroaluminum phthalocyanine based molecular switch, Physical Chemistry Chemical Physics 19 (2017) 22401–22405.